ARTICLE
Journal of Cellular Biochemistry 116:1080–1089 (2015)

Journal of Cellular Biochemistry

Inactivation of the Phosphatidylinositol 3-Kinase/Akt Pathway is Involved in BMP9-mediated Tumor-suppressive Effects in Gastric Cancer Cells

Liang Duan,[1] Liwei Ye,[1] Rui Wu,[2] Haiyan Wang,[1] Xueru Li,[1] Huan Li,[1] Shimei Yuan,[1] He Zha,[1] Hui Sun,[1] Yunyuan Zhang,[1] Xian Chen,[1] Yan Zhang,[1] and Lan Zhou[1]*

[1]*Key Laboratory of Diagnostic Medicine Designated by the Chinese Ministry of Education, College of Laboratory Medicine, Chongqing Medical University, Chongqing 400016, China*

[2]*Department of Laboratory Medicine, The First Affiliated Hospital of Chongqing Medical University, Chongqing 400016, China*

ABSTRACT

Bone morphogenetic proteins (BMPs) are members of the TGF-β superfamily signaling factors. Expression of several BMPs (BMP2, BMP4, and BMP7) is correlated to poor prognosis in gastric cancer patients. The function of BMP9, the latest discovered and most powerful osteogenetic factor, in gastric cancer is relatively unclear. In this report, we investigated the expression, function and underlying molecular mechanisms of BMP9 in gastric cancer. The results show that BMP9 expression was markedly decreased in gastric cancer tissues and cell lines. Enforced BMP9 expression in the gastric cancer cell lines SGC-7901 and MNK-45 increased apoptosis and reduced viability and migration. The in vivo function of BMP9 was evaluated in a xenograft mouse model. Tumors derived from SGC-7901 cells with enforced BMP9 expression (SGC-7901/BMP9) showed significantly reduced size and weight compared to that from control cells. Enforced BMP9 expression resulted in decreased Akt activity shown as lower levels of phosphorylation at Ser473 and Thr308 in Akt. The PI3K/Akt inhibitor LY294002 potentiated BMP9's viability and migration suppression, and apoptosis induction, which was associated with reduced expression of snail and VEGF and increased expression of E-cadherin. In addition, tumors derived from SGC-7901/BMP9 showed reduced Akt activity and VEGF expression, and increased E-cadherin expression. Therefore, our studies reveal for the first time that inhibition of the PI3K-Akt pathway is involved in the tumor suppressor effects of BMP9 in gastric cancer. J. Cell. Biochem. 116: 1080–1089, 2015.

KEY WORDS: BONE MORPHOGENIC PROTEINS 9; VIABILITY; APOPTOSIS; MIGRATION; GASTRIC CANCER

Gastric cancer is one of the most common malignant diseases that have high morbidity and mortality [Siegel et al., 2013; Uyama et al., 2013]. Although recent diagnostic and therapeutic advances have provided improved survival in early gastric cancer patients, high recurrence and poor prognosis remain the main problem in patients with advanced cancer. Accumulating evidence shows that multiple genetic and cell signaling alterations are highly related to gastric carcinogenesis [Tahara et al., 1993; Yasui et al., 2005]. Therefore, identifying key factors that participate in carcinogenesis may lead to new diagnostic, therapeutic and preventive approaches against gastric cancer.

Bone morphogenetic proteins (BMPs) are growth and differentiation factors belonging to the transforming growth factor-β superfamily. More than 20 BMPs have been identified thus far. They act as multifunctional regulators in a wide range of cellular responses, including cell proliferation, differentiation, adhesion, migration, and apoptosis [Feng and Derynck, 2005; David et al., 2009; Wagner et al., 2010]. BMPs have been indicated in the progression of several tumors

Conflicts of interest: None.
Liang Duan and Liwei Ye contributed equally to this work.
Grant sponsor: National Program on Key Basic Research Project of China; Grant number: 2011CB707906; Grant sponsor: Natural Science Foundation of China; Grant number: 30772548.
*Correspondence to: Prof. Lan Zhou, Key Laboratory of Diagnostic Medicine Designated by the Chinese Ministry of Education, College of Laboratory Medicine, Chongqing Medical University, No. 1 of Yixueyuan Road, Yuzhong District, Chongqing 400016, China. E-mail: zhoulan0111@foxmail.com
Manuscript Received: 30 April 2014; Manuscript Accepted: 18 December 2014
Accepted manuscript online in Wiley Online Library (wileyonlinelibrary.com): 5 January 2015
DOI 10.1002/jcb.25063 • © 2015 Wiley Periodicals, Inc.

including breast cancer, prostate cancer, lung cancer, colorectal cancer, melanoma, osteosarcoma [Ye et al., 2007]. Of note, the aberrant BMPs expression has been indicated in gastric cancer. The elevated expression of BMP2, BMP4, and BMP7 has been seen in gastric cancer, which is correlated to poor prognosis [Katoh and Terada, 1996; Park et al., 2008; Aoki et al., 2011]. Apart from the aberrant expression of BMPs, BMP downstream signaling cascades are also indicated in the development and progression of gastric cancer [Kuga et al., 2003; Bleuming et al., 2007].

BMP9, a new member of the BMP family, is reported to be as the most powerful osteogenetic factor [Cheng et al., 2003]. Recently, BMP9 has been demonstrated to play different roles in tumor progression. BMP9 inhibits proliferation, migration and invasiveness in prostate cancer cells, breast cancer cells and osteosarcoma cells, while it promotes the proliferation of ovarian cancer cells [Ye et al., 2008; Herrera et al., 2009; Wang et al., 2011; Lv et al., 2013]. However, the role of BMP9 in gastric cancer has not been well studied.

Epithelial-mesenchymal transition (EMT) is a phenomenon that epithelial cells of the primary tumor undergo a series of phenotypic changes, such as reduction of cell-cell adhesion, increment in cell mobility and invasiveness, loss of epithelial markers, and acquisition of mesenchymal phenotype, which contribute to cancer progression and metastasis [Guarino, 1995]. And aberrant EMT activation is closely associated with gastric carcinogenesis and tumor progression, which provides potential target for gastric cancer therapy [Katoh, 2005]. It has been shown that phosphatidylinositol-3-kinase/protein kinase B (PI3K/Akt) pathway was enable to produce transcription factor snail and to repress the transcription of the E-cadherin gene, leading to conversion of epithelial to mesenchymal phenotype [Lee et al., 2011]. Further, recent studies also showed that PI3K/AKT pathway is activated and significantly associated with the development, progression and metastasis of gastric cancer [Liu et al., 2010; Gu et al., 2014; Tapia et al., 2014]. One study also indicated that inhibition of the PI3K/Akt pathway suppresses growth and metastasis of gastric cancer [Ye et al., 2012]. Therefore, PI3K/Akt pathway may be a promising target for potential anti-gastric cancer therapeutic agents.

In our present study, we report that BMP9 expression is decreased in gastric cancer tissues and cell lines. Enforced BMP9 expression in gastric cancer cell lines promotes apoptosis and inhibits viability and migration in vitro, and suppresses tumor growth in a xenograft mouse model. We further provide evidence suggesting that inhibition of the PI3K-Akt pathway underlies the mechanism of BMP9's inhibitory effects on viability and migration in gastric cancer. Our results highlight the significance of BMP9 in the progression of gastric cancer, which implicate that BMP9 could be a potential therapeutic target for gastric cancer treatment.

MATERIALS AND METHODS

TISSUES

Fresh gastric cancer tissues and matched distal normal tissues were collected from 8 patients who had undergone gastric resection at the First Affiliated Hospital, Chongqing Medical University. The patients had not received chemotherapy, hormonal therapy, nor radiotherapy before surgery. Written informed consents were received from all participants. This study was approved by the Ethics Committee of Chongqing Medical University. Fresh samples from these patients were stored at −80°C and were used for reverse transcription-polymerase chain reaction and Western blot analysis. A part of each specimen was also fixed in 10% buffered-formalin, embedded in paraffin blocks and serially sectioned for hematoxylin-eosin (H-E) and immunohistochemical staining.

CELL LINES

Human gastric cancer cell lines SGC-7901 and MNK-45 were purchased from ATCC (American Type Culture Collection, Manassas, VA). Human gastric mucosal epithelial cell line GES-1 and embryonic kidney cell line 293 (HEK 293) were purchased from CCTCC (China Center for Type Culture Collection). SGC-7901, MNK-45, GES-1 and HEK293 cells were maintained in Dulbecco's modified Eagle's medium (DMEM) with 10% FBS (Hyclone). Cell culture was maintained at 37 °C in a humid atmosphere containing 5% CO_2.

REAGENTS AND ANTIBODIES

Anti-BMP9 (Cat no. 130703), anti-Cleaved-caspase-3 (Cat no. 22171-R), anti-VEGF (Cat no.7269), anti-E-cadherin (Cat no.7870), anti-PCNA (Cat no.7907), anti-β-actin (Cat no. 47778) antibodies and the specific PI3K inhibitor LY294002 were obtained from Santa Cruz Biotechnology, Inc.. Anti-Akt (Cat no.YT0178) and anti-phospho-Akt (Ser473) (Cat no.YP0006) antibodies were purchased from ImmunoWay, Inc.. Anti-phospho-Akt (Thr308) (Cat no.2965) antibody was purchased from Cell Signaling Technology, Inc..

RNA ISOLATION AND SEMI-QUANTITATIVE RT-PCR

Total RNA was extracted from both fresh frozen tissues and cells using Trizol (Invitrogen, Carlsbad, CA, USA). Semi-quantitative reverse transcriptase polymerase chain reaction (RT-PCR) was carried out as described by using the Takara RNA PCR kit. Primers were synthesized by Invitrogen. The mRNA levels of BMP9, snail, E-cadherin and VEGF were detected by RT-PCR. GAPDH was used as an endogenous control. The PCR primers were designed by using the Primer3 program (Table 1). The PCR products were separated in 1.5% agarose gels and stained with Good View™ (SBS Genetech, Beijing, China). The results were recorded with the Gel imaging system (Gel Doc 1000, Bio-Rad, USA) and Quantity One Version 4.5.0.

IMMUNOHISTOCHEMISTRY (IHC)

The expression of BMP9, PCNA, phospho-Akt (Thr308 and Ser473), cleaved-caspase-3, E-cadherin and VEGF in tissues was examined by IHC. The sections from the formalin fixed and paraffin-embedded tissues were deparaffinized and dehydrated. Then the sections were boiled for 10 min in 0.01 M citrate buffer and incubated with 0.3% hydrogen peroxide (H_2O_2) in methanol for 15 min to block endogenous peroxidase. The sections were then incubated with the anti-BMP9 antibody (1:200 dilution), anti-Cleaved-caspase-3 antibody (1:200 dilution), anti-phospho-Akt (Ser473) antibody (1:200 dilution), anti-phospho-Akt (Thr308) antibody (1:200 dilution), anti-VEGF antibody (1:200 dilution), anti-E-cadherin

TABLE 1. Primers Used in RT-PCR

Gene	Primer sequences	
	Forward	Reverse
BMP9	5′-CTGCCCTTCTTTGTTGTCTT-3′	5′-CCTTACACTCGTAGGCTTCATA-3′
Snail	5′-ACCCCACATCCTTCTCACTG-3′	5-TACAAAAACCCACGCAGACA-3′
E-cadherin	5′-CTGAGAACGAGGCTAACG-3′	5′-GTCCACCATCATCATTCAATAT-3′
VEGF	5′-GCACCCATGGCAGAAGGAGGAG-3′	5′-GTGCTGACGC-TAACTGACC-3′
GAPDH	5′-CAGCGACACCCACTCCTC-3′	5′-TGAGGTCCACCACCCTGT-3′

antibody (1:200 dilution), anti-PCNA antibody (1:200 dilution) overnight at 4 °C, following incubated with secondary antibody tagged with the peroxidase enzyme for 30 min at room temperature and were visualized with 0.05% 3,3-diaminobenzidine tetrachloride (DAB) till the desired brown reaction product was obtained. The sections were finally counterstained with hematoxylin. The negative control group was carried out with the same steps as described above except replacing the primary antibody with PBS. All slides were observed under a Nikon E400 Light Microscope and representative photographs were taken.

PRODUCTION AND INFECTION OF RECOMBINANT ADENOVIRUSES

The GFP-expressing adenovirus (pAdtrack-CMV/GFP) carrying GFP gene and recombinant BMP9-expressing adenovirus vehicles (pAdtrack-CMV/BMP9) carrying BMP9 gene were kindly presented by T.C He (Medical center, The University of Chicago), and all these adenoviruses were amplified in HEK293 cells before use [He et al., 1998; Wang et al., 2011; Lv et al., 2013]. The SGC-7901 and MNK-45 cells were infected with BMP9-expressing adenovirus (AdBMP9) or the control GFP-expressing adenovirus (AdGFP). A blank control group not infected with adenovirus was also included. After 8–12 h of culture, the medium was replaced with a fresh medium DMEM. The fluorescence was then observed 24 h later. The adenovirus-infected cells were used for subsequent experiments.

IMMUNOCYTOCHEMISTRY (ICC)

The cells were plated and cultured onto cleaned-up cover slips. After infected with and without AdGFP or AdBMP9 for indicated time, the cells were treated with 0.03% H_2O_2 for 5 min and incubated with anti-BMP9 antibody (1:200 dilution), following incubated for 30 min with secondary antibody tagged with the peroxidase enzyme and then visualized with 0.05% DAB until the desired brown reaction product was obtained. Finally, all sections were dehydrated, cleared and mounted in a neutral gum under cover slips. The negative control group was carried out with the same steps as described above except replacing the primary antibody with PBS. The staining of samples was observed under a Nikon E400 Light Microscope and representative photographs were taken.

CELL VIABILITY ASSAY

Cell viability was measured using MTT assay. Cells (3×10^3) were seeded into each well of 96-well culture plates, grown for 24 h, then infected with AdBMP9 and AdGFP (control for AdBMP9) in DMEM containing 1% FBS for the following 5 days. After the indicated time, the MTT reagent (Progema, Madison, WI) was added (10 μl/well) and incubated for 4 h at 37 °C. Medium was removed, the reduced MTT was solubilized in 100 μl per well of DMSO, and measured absorbance at 492 nm. Each condition was done in quintuplicate, and the overall experiment was repeated thrice.

TUMORIGENICITY ASSAYS IN NUDE MICE

The in vivo experiment was performed in accordance with the guidelines established by the Animal Care and Use Committee, University Laboratory Animal Research. The 4–6-week old female nude mice were randomly divided into 3 groups (n = 4/group). About one week later, Untreated, AdGFP-infected and AdBMP9-infected SGC-7901 cells (1×10^8/each nude mouse) were suspended in 200 μl phosphate buffer solution (PBS), and then were injected subcutaneously into the posterior flank position of nude mice. Subcutaneous tumor growth was recorded every 4 days with vernier calipers. Tumor volume was calculated using the formula: $\pi/6 \times (R\ max \times R\ min^2)$, where R = tumor diameter. The mice were sacrificed after 44 days, and the tumor tissues were collected and stored at -80 °C and were used for Western blot analysis. In addition, the tissue specimens were also fixed in 10% buffered-formalin, embedded in paraffin blocks and serially sectioned for immunohistochemical analysis. The in vivo experiment was performed twice.

APOPTOSIS ASSAYS

Hoechst 33258 staining was used to evaluate the apoptosis of gastric cancer cells. Gastric cancer cells were infected with and without AdGFP and AdBMP9 for 24 h or 48 h and washed with PBS for 3 times. Hoechst 33258 at 10 μg/ml (Santa Cruz Biotechnology, Santa Cruz, CA) was added to the solution and incubated at 37 °C for 30 min, and observed under an inverted fluorescence microscope.

Annexin V-PI staining was also used to evaluate the apoptosis of gastric cancer cells. Annexin V—FITC apoptosis kit were purchased from Becton Dickinson (San Diego, CA). The cells were harvested after treatment, washed twice with pre-chilled PBS and resuspended in 1× binding buffer at a concentration of 1×10^6 cells/ml. One hundred microliter of the cell suspension (1×10^5 cells) was mixed with 5 μl of Annexin V-FITC and 5 μl of propidium iodide according to the manufacturer's instruction. The mixed solution was gently vortexed and incubated in dark at room temperature (25°C) for 15 min. Four hundred microliter of 1× dilution buffer was then added to each tube and apoptosis analysis was performed by FACSCalibur flow cytometer within 1 h.

Apoptosis was also determined immunohistochemically by the terminal deoxynucleotidyltransferase-mediated dUTP nick end labeling (TUNEL) assay in formalin-fixed tissues using an In Situ Cell Death Detection Kit, POD (Roche Diagnostics, Indianapolis, IN)

as per manufacturer's instructions. Positive control was generated by the treatment of samples with DNase I.

CELL MIGRATION ASSAY

Cell migratory ability was analyzed by transwell migration assay using 24-well culture inserts without any extracellular matrix component. The transwell migration assay was performed as previously described [Duan et al., 2013]. The cells were seeded in the upper chamber of 24-well culture inserts, and DMEM supplemented with 20% FBS was added to the lower chamber as a chemoattractant. After 24 h, the cells were dried for 5 min, fixed with dehydrated alcohol, and stained with hematoxylin-eosin. The cells that penetrated the pore filter were counted. Mean values for five randomly selected fields were obtained for each well. The experiments were performed and repeated thrice.

WESTERN BLOT ASSAY

The cells or tissues were collected and lysed on ice in a RIPA buffer. The total lysate was centrifuged and the proteins in the supernatant were quantitated by BCA (bicinchoninic acid) assay and denatured by boiling and loaded onto 10% SDS-PAGE. Then the electrophoretic gel that contained interest and control proteins was cropped per the molecular size markers, and the cropped gels were blotted onto the PVDF membranes. Then the membranes were blocked with 5% bovine serum albumin at room temperature for 2 h and incubated with anti-phospho-Akt (Thr308) antibody (1:1000 dilution), or anti-phospho-Akt (Ser473) antibody (1:1000 dilution), or anti-Akt antibody (1:1000 dilution), anti-PCNA antibody (1:1000 dilution), or anti-cleaved caspase-3 antibody (1:1000 dilution), or anti-E-cadherin antibody (1:1000 dilution), or anti-β-actin antibody (1:1000 dilution). The secondary antibodies included goat anti-rabbit IgG serum or goat anti-mouse IgG serum. The proteins of interest were detected using the SuperSignal West Pico Chemiluminescent Substrate kit. The results were recorded using the Bio-Rad Electrophoresis Documentation (Gel Doc 1000) and Quantity One version 4.5.0 software.

STATISTICAL ANALYSIS

All values in the text and figures are presented as the means ± standard deviation (SD). The differences were analyzed by one-way ANOVA followed by the Student-Newman-Keuls test, and all statistical analyses were performed using GraphPad Prism software (GraphPad Software, La Jolla, CA). Statistical differences are presented at probability levels of $P < 0.05$, $P < 0.01$, and $P < 0.001$.

RESULTS

DECREASED EXPRESSION OF BMP9 IN HUMAN GASTRIC CANCER TISSUS AND CELL LINES

BMP9 mRNA was detected in samples from 8 patients with gastric cancer by RT-PCR, which showed decreased expression of BMP9 mRNA in the gastric cancer tissues compared to the matched distal normal gastric tissues (Fig. 1A and B). Furthermore, decreased BMP9 expression on protein level in gastric cancer tissues was confirmed by IHC, which strongly detected BMP9 in glandular epithelial cells in matched distal normal gastric tissues but barely in tumor cells (Fig. 1C).

The mRNA and protein levels of BMP9 in gastric cancer cell lines SGC-7901 (with low malignancy) and MNK-45 (with high malignancy) were compared to that in the normal gastric mucosal epithelial cell line GES-1. BMP9 mRNA expression was detected in GES-1 cells but barely in both two gastric cancer cell lines by RT-PCR (Fig. 1D and E). Similar result of BMP9 protein expression was confirmed by ICC (Fig. 1F). Thus, we enforced BMP9 expression in the two gastric cancer cell lines with adenovirus vectors expressing BMP9 (AdBMP9) for the following studies. Enforced expression of BMP9 mRNA and protein was confirmed by RT-PCR and ICC, respectively (Fig. 1D, E and F).

BMP9 INHIBITS VIABILITY AND INDUCES APOPTOSIS IN HUMAN GASTRIC CANCER CELL LINES

Cell viability was assayed by MTT-assay. AdBMP9-mediated of enforced BMP9 expression in SGC-7901 cells attenuated cell viability (Fig. 2A). Similar result was also obtained from MNK-45 cells (Fig. 2B). It is likely that the reduced viable cells by BMP9 expression was partly due to suppressed cell proliferation, because the decreased PCNA expression in the two enforced BMP9 expression cell lines was detected by Western blot (Fig. 2C).

To determine whether BMP9-induced cell viability reduction involves apoptosis, Hoechst 33258 staining was performed. Seventy-two hours after enforced BMP9 expression by infecting SGC-7901 cells and MNK-45 cells with AdBMP9, apoptotic cell numbers were significantly increased compared to that of the control AdGFP groups (Fig. 2D). This result was further confirmed by flow cytometric analysis with annexin V-PI staining, showing that apoptosis rates of SGC-7901 cells and MNK-45 cells were prominently increased when compared to that of the control AdGFP groups (Fig. 2E).

INACTIVATION OF PI3K/AKT PATHWAY IS INVOLVED IN BMP9-INDUCED VIABILITY REDUCTION AND APOPTOSIS ACTIVATION

As the PI3K/Akt pathway plays a critical role in cancer cell viability, apoptosis and cancer progression, we examined the effect of BMP9 on this cell survival pathway. SGC-7901 and MNK-45 cells infected with and without AdBMP9 and AdGFP were cultured for 24 h, 72 h, and 96 h, phosphorylation at Ser473 and Thr308 sites of Akt was detected by Western blot. The results showed that of enforced BMP9 expression in SGC-7901 and MNK-45 cells led to decreased phosphorylation at Ser473 and Thr308 while the total Akt level was unaffected (Fig. 3A). We then investigated the possible role of BMP9-induced decreased Akt activity in viability and apoptosis. The specific PI3K inhibitor LY294002 (20 μM) which partially inhibited Akt phosphorylation was used in the following studies (Fig. S1). The AdBMP9-infected SGC-7901 and MNK-45 cells were treated with LY294002 for 72 h and 96 h, and cell viability and apoptosis were measured. The results showed that BMP9 and LY294002 cooperatively potentiated the viability suppression (Fig. 3B and C) and apoptosis promotion (Fig. 3D, E and F). These data indicate that suppression of the PI3K/Akt pathway activity contributes to BMP9-induced viability decrease and apoptosis increase in gastric cancer cells.

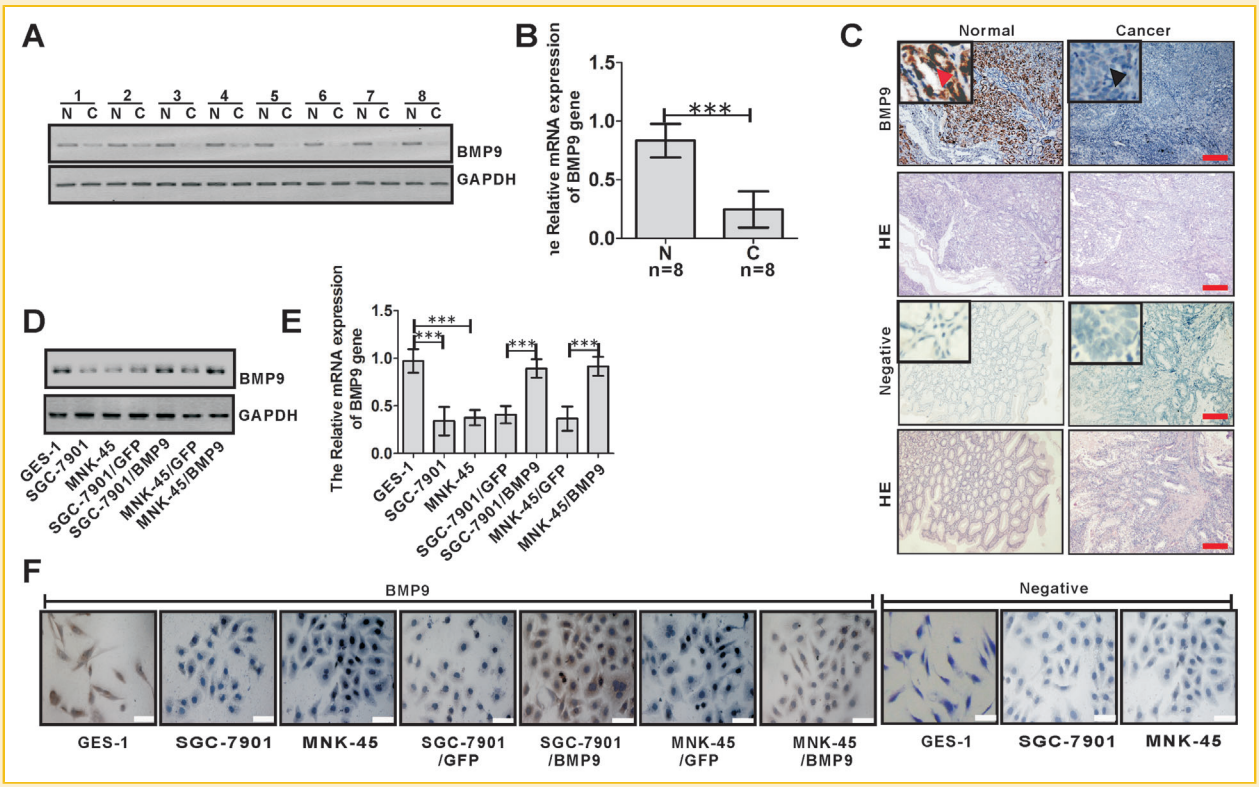

Fig. 1. Decreased BMP9 expression in human gastric cancer tissues and cell lines and the validation of AdBMP9. A: RT-PCR for BMP9 mRNA expression in gastric cancer tissues (C) and matched distal normal tissues (N) from eight patients. GAPDH was detected as an input control. B: The relative mRNA expression of BMP9 gene is quantified by BMP9/GAPDH densitometric ratios in gastric cancer tissues (C) and matched distal normal tissues (N) from eight patients. ***$P < 0.001$, N vs. C. C: BMP9 was detected by IHC. The specificity of anti-BMP9 antibody was checked by replacing it with negative control PBS. Red scale bars, 500 μm; HE, hematoxylin and eosin staining. Red triangle: BMP9-expressing glandular epithelial cells (brown); black triangle: BMP9-expressing tumor cells (brown). D and E: BMP9 mRNA expression (D) in uninfected (SGC-7901 and MNK-45), AdGFP-infected (SGC-7901/GFP and MNK-45/GFP) and AdBMP9-infected (SGC-7901/BMP9 and MNK-45/BMP9) gastric cancer cell lines and a normal gastric mucosal epithelial cell line (GES-1) was detected by RT-PCR, and its relative expression (E) is quantified by BMP9/GAPDH densitometric ratios. *** $P < 0.001$, GES-1 vs. SGC-7901 or MNK-45; SGC-7901/BMP9 vs. SGC-7901/GFP; MNK-45/BMP9 vs. MNK-45/GFP. F: As mentioned in D, BMP9 protein expression in these cell lines is detected by ICC. The negative control was carried out with PBS. White scale bars, 100 μm.

INACTIVATION OF THE PI3K/AKT PATHWAY IS INVOLVED IN BMP9-INDUCED SUPRESSION OF CELL MIGRATION

Cell migration plays a crucial role in the process of tumor cell invasion and metastasis. The cells were infected with AdBMP9 for 24 h, and cell migration was analyzed by transwell migration assay. Enforced BMP9 expression in SGC-7901 and MNK-45 cells resulted in a significant reduction in cell migration as compared to that of control AdGFP-infected cells (Fig. 4A). Based on the suppressive role of BMP9 in cell viability, we then explore whether the decreased migration effect is due to the decreased viability by BMP9. Our result showed that BMP9 had no effect on viability in SGC-7901 and MNK-45 cells infected with AdBMP9 for 24 h (Fig. 4B).

As EMT underlies malignant cancer development and metastasis that enables cancer cells to depart from the primary tumor site, invade surrounding tissue and disseminate to distant organs. EMT molecular markers snail, E-cadherin and VEGF were detected in samples from 8 patients with gastric cancer by IHC, which showed decreased expression of E-cadherin and increased snail and VEGF in the gastric cancer tissues compared to the matched distal normal gastric tissues (Fig. S2). Given that BMP9 inhibits gastric cancer cell migration, we investigated the effect of BMP9 on EMT. The higher mRNA expression of E-cadherin in SGC-7901 and MNK-45 cells infected with AdBMP9 was detected by RT-PCR. In contrast, the decreased mRNA expression of snail and vascular endothelial growth factor (VEGF) was observed in AdBMP9-infected cells (Fig. 4C, D and E).

We further verified the role of PI3K/Akt in BMP9-induced cell migration suppression. SGC-7901 and MNK-45 cells infected with AdBMP9 were treated with LY294002 for 24 h and cell migration was measured. While BMP9 significantly reduced cell migration, LY294002 pronouncedly enhanced this effect of BMP9 (Fig. 4A). In addition, no effect on viability was observed in Ad-BMP9 infected SGC-7901 and MNK-45 cells treated with LY294002 for 24 h (Fig. 4B), suggesting that the reduced migration effect was not due to the decreased viability. In addition, BMP9 and LY294002 pronouncedly increased E-cadherin expression and decreased snail and VEGF expression (Fig. 4C, D and E). These results suggest that inhibition of the PI3K/Akt pathway plays a critical role in regulating BMP9-mediated decreased migration in gastric cancer cells.

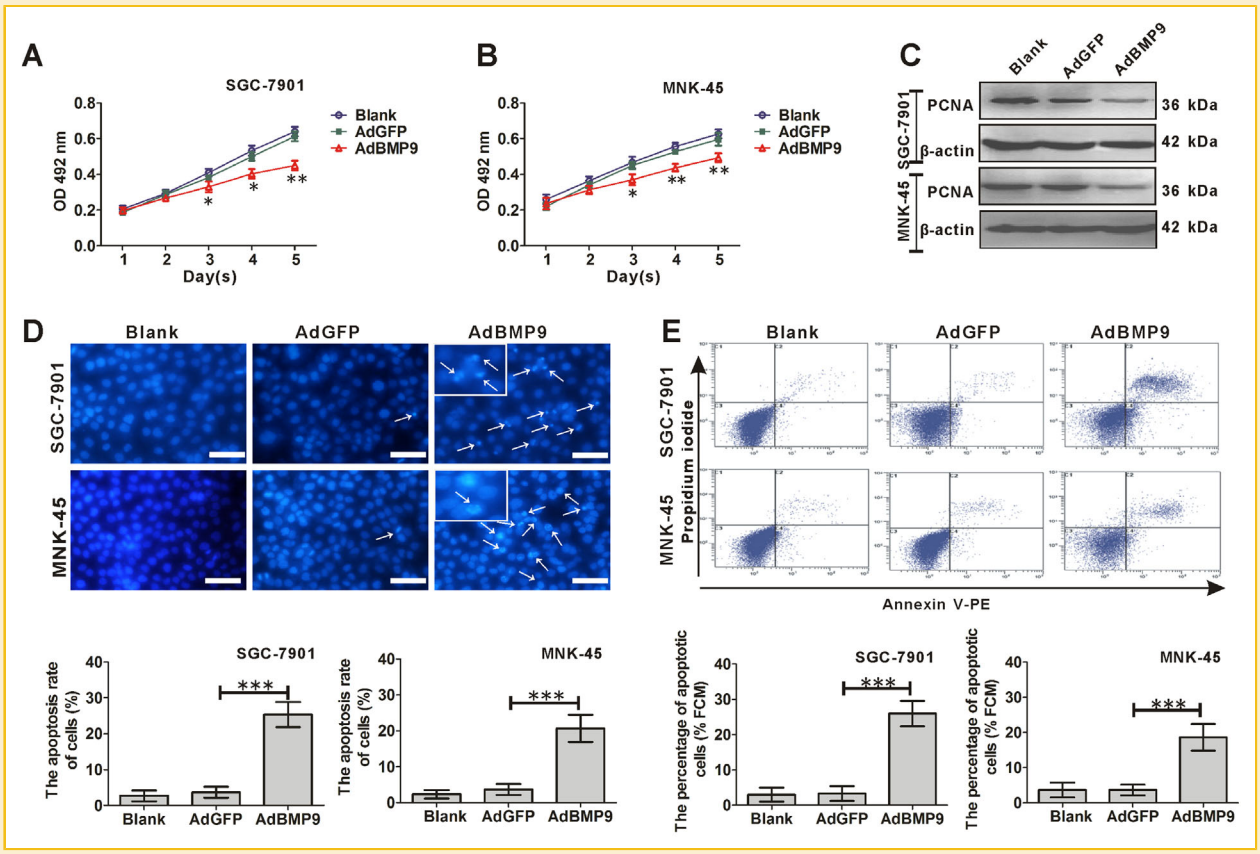

Fig. 2. The effect of BMP9 on the viability and apoptosis in gastric cancer cells. A and B: SGC-7901 (A) and MNK-45 (B) cells were infected with AdGFP or AdBMP9 continuously cultured for five days, and cell viability was detected by the MTT-assay. Results are expressed as the mean absorbance ± SD of three independent experiments. $^{*}P < 0.05$, $^{**}P < 0.01$, AdBMP9 vs. AdGFP control. C: PCNA expression was detected in lysates of SGC-7901 and MNK-45 cells infected with and without AdGFP or AdBMP9 for 72 h by Western blot. β-actin was detected as an input control. D: SGC-7901 and MNK-45 cells were infected with AdGFP or AdBMP9 for 72 h, and apoptosis was detected by hoechst 33258 staining. Apoptosis rate of the SGC-7901 and MNK45 cells was quantified in lower panels. White arrow: apoptotic cells. Apoptosis rate was calculated as: (apoptotic cell number / total cell number) ×100%. White scale bars, 100 μm. $^{***}P < 0.001$, AdBMP9 vs. AdGFP. E: Cells double stained with AnnexinV/PI after infection with and without AdGFP or AdBMP9 for 72 h were analyzed by flow cytometry. The percentage of apoptotic cells was quantified in the lower panels. $^{***}P < 0.001$, AdBMP9 vs. AdGFP.

BMP9 INHIBITS TUMORIGENICITY OF GASTRIC CANCER CELLS IN VIVO

We further investigated the effect of BMP9 on growth of gastric cancer xenograft tumors in vivo. The 3 groups of SGC-7901 cells (untreated, AdGFP-infected, and AdBMP9-infected) were subcutaneously implanted in nude mice. Tumors became palpable from day 20 to 40 and continued to grow. While the tumors derived from the SGC-7901/GFP grew in a speed comparable to that of tumors from the untreated SGC-7901 cells, the tumors derived from the SGC-7901/BMP9 cells had a much lower growth rate (Fig. 5A). There was decreased expression of PCNA by IHC and Western blot analysis and hence, reduced mitotic index in the AdBMP9-infected group (Fig. 5B, C and G). Of note, histological examination by hematoxylin eosin (H-E) staining showed that the tumor cells in SGC-7901/BMP9 group had the characteristic morphological changes of apoptosis, with the concentrated cytoplasm, hyperchromatic and pyknotic nucleus (Fig. 5B). In addition, apoptosis was also evaluated by TUNEL staining, which showed a higher percentage of TUNEL-positive tumor cells and hence, increased apoptosis index in the SGC-7901/BMP9 group (Fig. 5B and D). A higher expression of active (cleaved) caspase-3 by IHC (Fig. 5B) and western blot (Fig. 5G) analysis further confirmed that apoptosis was increased in the SGC-7901/BMP9 group.

Based on the decreased effect of BMP9 on Akt activity in gastric cancer cells in vitro, phosphorylation at Ser473 and Thr308 sites of Akt was detected in xenograft tumor tissues derived from SGC-7901/BMP9 group by IHC and Western blot analysis, which showed decreased phosphorylation of AKT at Ser473 and Thr308 (Fig. 5E and G). Further, increased E-cadherin and decreased VEGF protein expression was also confirmed in xenograft tumor tissues derived from SGC-7901/BMP9 (Fig. 5 F and G).

DISCUSSION

BMPs are multifunctional cytokines that modulate the growth, differentiation and apoptosis of various cell types [Wang, 1993; Singh and Morris, 2010; Kopf et al., 2013]. Recently, BMPs, BMP receptors and their downstream signaling molecules have been linked to carcinogenesis and tumor progression. Aberrant BMPs (BMP2, BMP4, and BMP7) expression and its association with

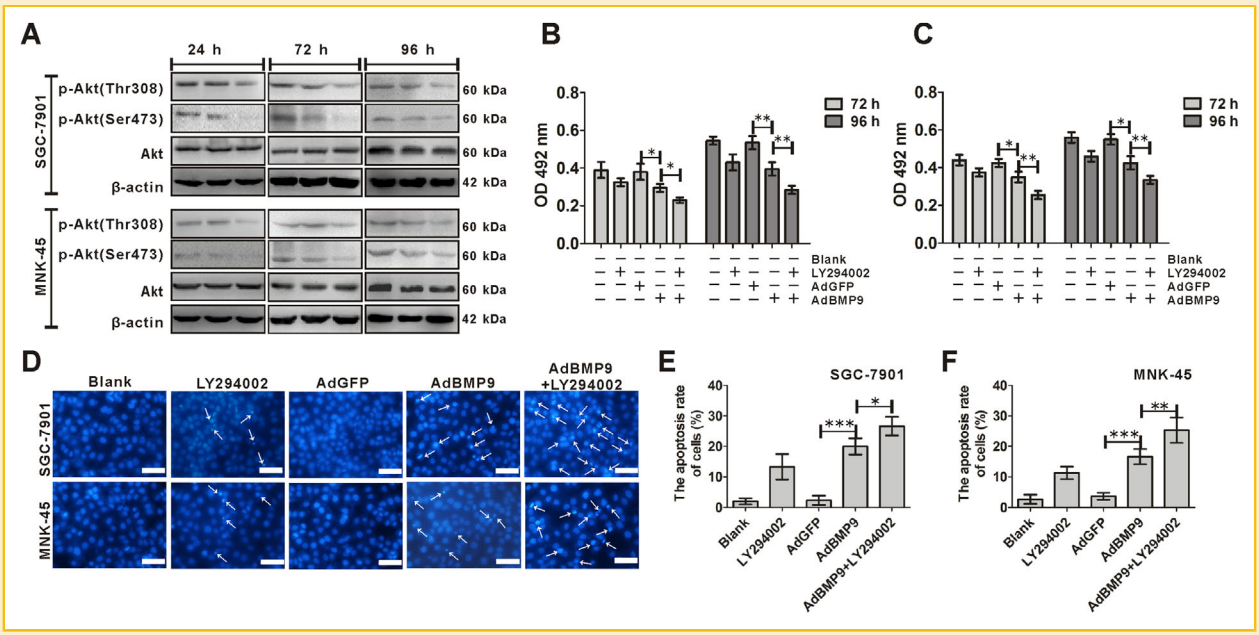

Fig. 3. Inhibition of PI3K/Akt activity is involved in BMP9-induced viability reduction and apoptosis activation. A: Akt phosphorylation at Ser473 and Thr308 was detected by Western blot in SGC-7901 or MNK-45 cells infected with AdGFP or AdBMP9 for 24 h, 72 h, and 96 h. Total Akt and β-actin were detected as loading controls. B and C: The effect of LY294002 on BMP9-induced viability of SGC-7901 (B) and MNK-45 (C) cells. The cells were infected with AdBMP9 followed by treatment with LY294002 (20 μM) for 72 h and 96 h, and cell viability was measured by MTT assay. Results are expressed as mean ± SD of absorbance of three independent experiments. $^{*}P < 0.05$ (72 h), AdBMP9 vs. AdGFP, AdBMP9 vs. AdBMP9 + LY294002; $^{**}P < 0.01$ (72 h), AdBMP9 vs. AdBMP9 + LY294002; $^{*}P < 0.05$ (96 h), AdBMP9 vs. AdGFP; $^{**}P < 0.01$ (96 h), AdBMP9 vs. AdGFP, AdBMP9 vs. AdBMP9 + LY294002. D: The effect of LY294002 on BMP9-induced cell apoptosis in SGC-7901 and MNK-45 cells was detected by hoechst 33258 staining. The cells were infected with AdBMP9 followed by treatment with LY294002 (20 μM) for 72 h, and apoptosis was detected by hoechst 33258 staining. White arrow: apoptotic cells. E and F: Apoptosis of SGC-7901 and MNK-45 in D was quantified. The apoptosis rate was calculated as: (apoptotic cell number / total cell number) ×100%. White scale bars, 100 μm. $^{*}P < 0.05$ and $^{**}P < 0.01$, AdBMP9 vs. AdBMP9 + LY294002; $^{***}P < 0.001$, AdBMP9 vs. AdGFP.

disease progression and poor prognosis have been reported in gastric cancer [Katoh and Terada, 1996; Park et al., 2008; Aoki et al., 2011]. The expression and function of BMP-9, a new member of the BMP family, has not been reported in gastric cancer. In this report, we provide data demonstrating that BMP9 expression is decreased in gastric cancer and that inhibition of the PI3K-Akt pathway is involved in BMP9′s gastric cancer suppressing function.

Unlike increased expression of other numbers of BMPs such as BMP-2, BMP-4, and BMP-7 in gastric cancer shown in previous studies, our study demonstrates that BMP9 expression at both the mRNA and protein levels was reduced in gastric cancer tissues and cell lines, which is consistent with previous reports showing that BMP9 expression was decreased in various tumors such as prostate cancer, breast cancer and osteosarcoma [Ye et al., 2008; Wang et al., 2011; Lv et al., 2013]. Given its reduced expression in cancer cells, BMP9 is likely to be involved in carcinogenesis and a potent suppressor in gastric cancer progression.

To further study the role of BMP9 in gastric cancer development, enforced BMP9 expression was established in gastric cancer cell lines SGC-7901 and MNK-45. We show for the first time that BMP9 possesses a tumor-suppressive activity in gastric cancer. We observed reduced viability and increased apoptosis in SGC-7901/BMP9 and MNK-45/BMP9 cells in vitro. The in vitro function of BMP9 was also directly demonstrated in our studies with a xenograft mouse model. We observed a significant reduction in tumor growth, a lower mitotic index and a higher apoptosis index in tumors derived from SGC-7901/BMP9 cells in nude mice. Decreased viability and increased apoptosis in BMP9-expressing gastric cancer is consistent with previous studies showing BMP9 overexpression induces apoptosis in prostate cancer cells and inhibits proliferation in breast cancer and osteosarcoma cells [Ye et al., 2008; Wang et al., 2011; Li et al., 2012; Lv et al., 2013]. However, BMP9 was reported to stimulate ovarian cancer cell proliferation through the Smad pathway [Herrera et al., 2009]. The reason of discrepancy in the effects of BMP9 in various cancers is unclear but could be cancer type specific. It may also involve other undefined factors.

To explore the mechanisms underlie the tumor-suppressive role of BMP9, we focused on PI3K/Akt. The PI3K/Akt pathway regulates many of the hallmarks of cancer, including tumor cell growth, apoptosis and metastasis and is frequently dysregulated in tumor including gastric cancer [Larue and Bellacosa, 2005; Song et al., 2005; Wen et al., 2010; Bruhn et al., 2013]. Downregulation of Akt activity has been reported to mediate BMP9-induced suppression of osteosarcoma cell growth [Li et al., 2012]. In our studies, we found that enforced BMP9 expression partially suppressed Akt activity, which was measured by detection of phosphorylation at Ser473 and Thr308. Further, treatment with the PI3K/Aktinhibitor LY294002 potentiated BMP9-induced viability inhibition and apoptosis activation, suggesting that inactivation of the PI3K-Akt pathway is likely involved in BMP9's anti-tumor effect. Increased PI3K-Akt activity has been found in several types of cancers, which promotes cell survival and inhibits apoptosis through effects on

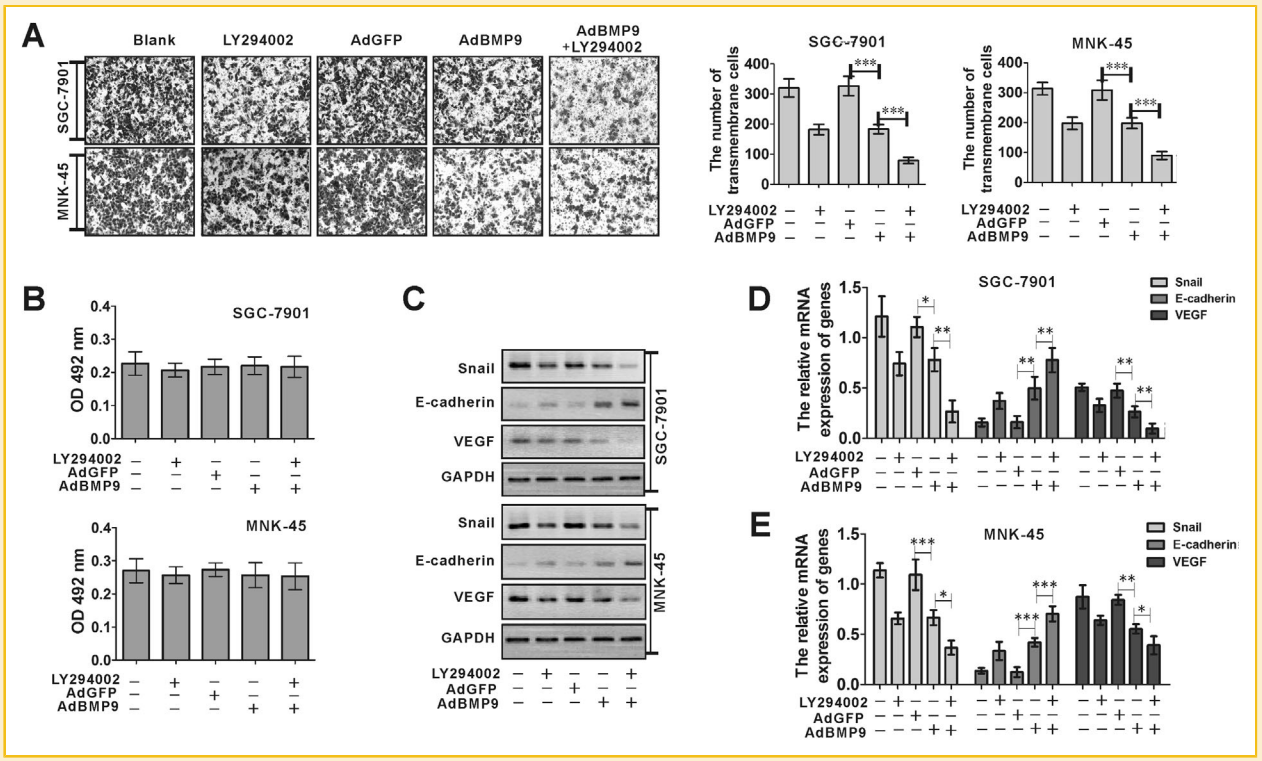

Fig. 4. Inhibition of the PI3K/Akt pathway activity is involved in BMP9-induced migration suppression. A: The cells were infected with AdBMP9 followed by treatment with LY294002 (20 μM) for 24 h, and cell migration was detected by transwell migration assay. The representative images of transmembrane cells are shown, the mean ± SD of migrated cell numbers per microscopic field of three independent experiments are quantified (right panel). Magnification, ×100. $^{***}P < 0.001$, AdBMP9 vs. AdGFP and AdBMP9 vs. AdBMP9 + LY294002. B: The cells were infected with AdBMP9 followed by treatment with LY294002 (20 μM) for 24 h, and cell viability was detected by MTT assay. Results are expressed as mean ± SD of absorbance of three independent experiments. C: The effect of LY294002 (20 μM) on BMP9-mediated mRNA expression of snail, E-cadherin and VEGF was analyzed by RT-PCR. D and E: The relative expression of snail, E-cadherin and VEGF in SGC-7901 (D) and MNK-45 (E) was quantified by snail or E-cadherin or VEGF/GAPDH densitometric ratios. GAPDH was detected as an input control. $^{*}P < 0.05$, $^{**}P < 0.01$ and $^{***}P < 0.001$, AdBMP9 vs. AdGFP or AdBMP9 vs. AdBMP9 + LY294002.

numerous downstream targets [Zhou et al., 2001; Julien et al., 2007; Qiao et al., 2008]. Abnormal activation of the PI3K-Akt pathway has also been reported in gastric cancer, and targeted blockade of this pathway may inhibit gastric cancer growth and metastasis involving down-regulation of Ki-67 and MMP-2 expression [Ye et al., 2012]. Downstream targets that are affected by BMP9-mediated PI3K-Akt suppression need to be investigated in the future.

We further show that enforced BMP9 expression inhibited the migration of gastric cancer cells, and downregulation of the PI3K-Akt pathway activity with LY294002 potentiated BMP9-induced migration suppression, suggesting that inactivation of PI3K-Akt is involved in this function of BMP9. These results are consistent with the reports that the PI3K-Akt pathway is important for migration in gastric cancer cells [Lin et al., 2007; Li et al., 2009; Ho et al., 2010]. We also observed EMT activation by through increased snail and decreased E-cadherin in gastric cancer tissues, which is in line with previous studies demonstrating EMT activation is closely associated with gastric carcinogenesis [Katoh, 2005]. Additionally, we show that inhibition of the PI3K-Akt pathway with LY294002 potentiated BMP9's inhibition of snail gene transcription and activation of E-cadherin gene transcription, suggesting that BMP9 suppresses migration and EMT of gastric cancer cells by downregulating the PI3K/Akt pathway. Altogether, these results suggest that inactivation of the PI3K-Akt pathway is involved in the BMP9-induced migration suppression in gastric cancer cells.

VEGF, an important regulator of tumor angiogenesis, has been reported to be a strong predictor of both metastasis and prognosis in gastric cancer [Cao et al., 2013; Chen et al., 2013; Kigure et al., 2013]. We confirmed its elevated expression by using IHC for detection of VEGF in gastric cancer tissues. Dysregulation of VEGF was reported to be through the PI3K-Akt pathway in tumors [Ma et al., 2009; Shafee et al., 2009; Liu et al., 2011; Tian et al., 2013]. We observed that enforced BMP9 expression resulted in reduced expression of VEGF gene and protein in gastric cancer cells both in vitro and in vivo, and inhibition of the PI3K-Akt pathway with LY294002 potentiated BMP9-induced VEGF suppression. Therefore, our data also imply that BMP9 may inhibit angiogenesis during gastric cancer metastasis by suppressing VEGF expression.

In summary, we demonstrate for the first time that BMP9 expression is decreased in gastric cancer tissues and cell lines, and that enforced BMP9 expression inhibits the viability and migration and promotes apoptosis in gastric cancer cells. We further show that the tumor-suppressing function of BMP9 through inhibiting the PI3K-Akt pathway. Our data provide important information for understanding the role of BMP9 in gastric cancer progression, which shed light on the mechanism of gastric carcinogenesis.

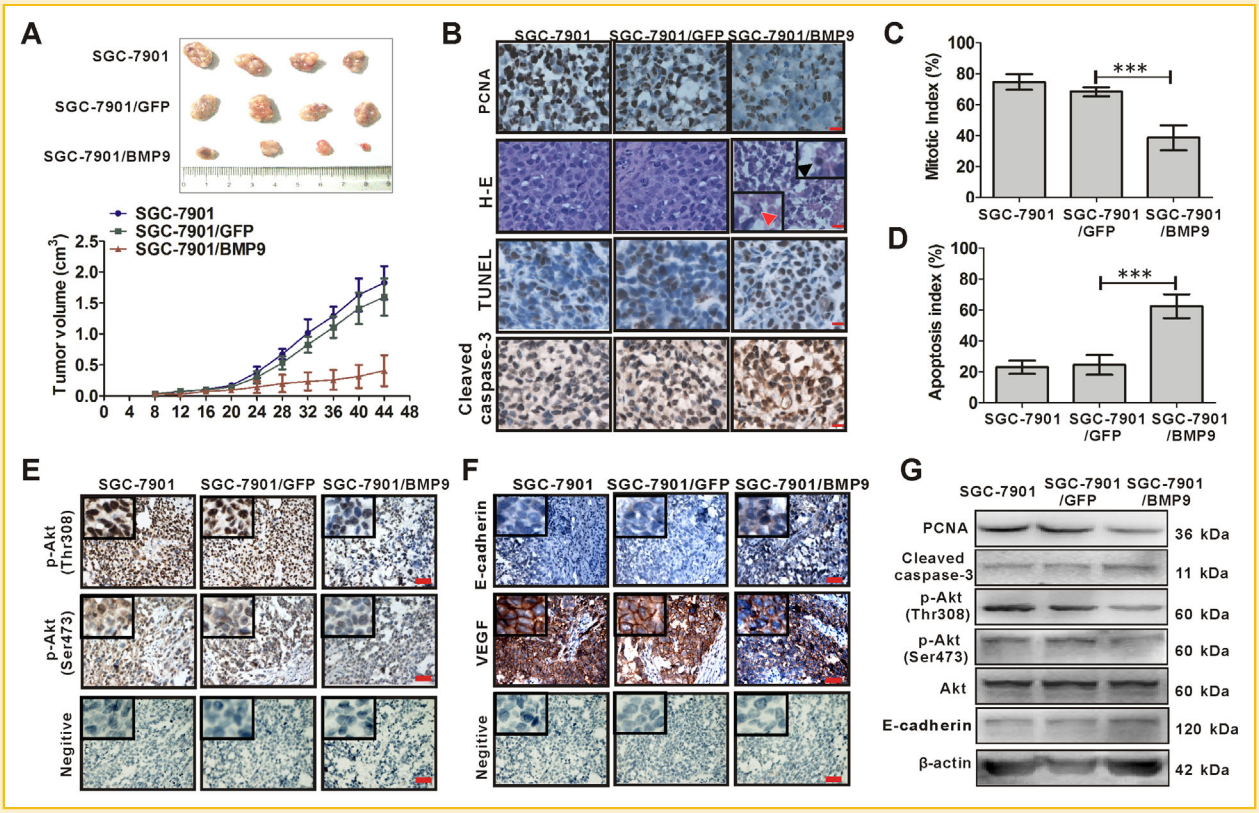

Fig. 5. The effect of BMP9 on xenografted tumor growth in vivo. A: Images of excised tumors derived from mice injected with SGC-7901, SGC-7901/GFP, and SGC-7901/BMP9 cells and tumor growth curves of all groups (SGC-7901, SGC-7901/GFP, SGC-7901/BMP9; n = 4/group). Tumor volume was measured every 4 days. B: H-E staining, TUNEL staining and IHC for PCNA and cleaved caspase-3 staining in representative fields on the tumor tissue slides from all groups. Red triangle: apoptotic cells (karyorrhexis); black triangle: apoptotic cells (pyknotic nucleus). Red scale bars, 50 μm. C: Mitotic index was calculated as the percentage of PCNA-positive cells in five random fields on the tumor tissue slides from all groups. $^{***}P < 0.001$, AdBMP9 vs. AdGFP. D: Apoptosis index was calculated as the percentage of TUNEL-positive cells in five random fields in the tumor tissue slides from all groups. $^{***}P < 0.001$, AdBMP9 vs. AdGFP. E and F: IHC for Akt phosphorylation at Ser473 and Thr308, E-cadherin and VEGF staining in representative fields on the tumor tissue slides from all groups. The negative control was carried out with PBS. Red scale bars, 100 μm. G: PCNA, cleaved caspase-3, p-Akt (Ser473 and Thr308), Akt, Ecadherin was detected by Western blot in lysate of representative tumor tissues from all groups. β-actin was detected as an input control.

ACKNOWLEDGMENTS

The authors would like to thank Professor T.C. He (The University of Chicago, Medical center) for kindly providing the AdBMP9 and AdGFP plasmids.

REFERENCES

Aoki M, Ishigami S, Uenosono Y, Arigami T, Uchikado Y, Kita Y, Kurahara H, Matsumoto M, Ueno S, Natsugoe S. 2011. Expression of BMP-7 in human gastric cancer and its clinical significance. Br J Cancer 104:714–718.

Bleuming SA, He XC, Kodach LL, Hardwick JC, Koopman FA, Ten Kate, van Deventer FJ, Hommes SJ, Peppelenbosch DW, Offerhaus MP, Li GJ, van den Brink L. 2007. Bone morphogenetic protein signaling suppresses tumorigenesis at gastric epithelial transition zones in mice. Cancer Res 67: 8149–8155.

Bruhn MA, Pearson RB, Hannan RD, Sheppard KE. 2013. AKT-independent PI3-K signaling in cancer - emerging role for SGK3. Cancer Manag Res 5:281–292.

Cao W, Fan R, Yang W, Wu Y. 2013. VEGF-C expression is associated with the poor survival in gastric cancer tissue. Tumour Biol.

Chen J, Tang D, Wang S, Li QG, Zhang JR, Li P, Lu Q, Niu G, Gao J, Ye NY, Wang DR. 2013. High expressions of galectin-1 and VEGF are associated with poor prognosis in gastric cancer patients. Tumour Biol.

Cheng H, Jiang W, Phillips FM, Haydon RC, Peng Y, Zhou L, Luu HH, An N, Breyer B, Vanichakarn P, Szatkowski JP, Park JY, He TC. 2003. Osteogenic activity of the fourteen types of human bone morphogenetic proteins (BMPs). J Bone Joint Surg Am 85-A:1544–1552.

David L, Feige JJ, Bailly S. 2009. Emerging role of bone morphogenetic proteins in angiogenesis. Cytokine Growth Factor Rev 20:203–212.

Duan L, Wu R, Ye L, Wang H, Yang X, Zhang Y, Chen X, Zuo G, Zhang Y, Weng Y, Luo J, Tang M, Shi Q, He T, Zhou L. 2013. S100A8 and S100A9 are associated with colorectal carcinoma progression and contribute to colorectal carcinoma cell survival and migration via Wnt/beta-catenin pathway. PLoS One 8:e62092.

Feng XH, Derynck R. 2005. Specificity and versatility in tgf-beta signaling through Smads. Annu Rev Cell Dev Biol 21:659–693.

Guarino M. 2007. Epithelial-mesenchymal transition and tumour invasion. Int J Biochem Cell Biol 39:2153–2160.

Gu Y, Jin S, Wang F, Hua Y, Yang L, Shu Y, Zhang Z, Guo R. 2014. Clinicopathological significance of PI3K, Akt and survivin expression in gastric cancer. Biomed Pharmacother 68:471–475.

He TC, Zhou S, da Costa LT, Yu J, Kinzler KW, Vogelstein B. 1998. A simplified system for generating recombinant adenoviruses. Proc Natl Acad Sci USA 95:2509–2514.

Herrera B, van Dinther M, Ten Dijke, Inman P. 2009. Autocrine bone morphogenetic protein-9 signals through activin receptor-like kinase-2/Smad1/Smad4 to promote ovarian cancer cell proliferation. Cancer Res 69:9254–9262.

Ho HH, Chang CS, Ho WC, Liao SY, Wu CH, Wang CJ. 2010. Anti-metastasis effects of gallic acid on gastric cancer cells involves inhibition of NF-kappaB activity and downregulation of PI3K/AKT/small GTPase signals. Food Chem Toxicol 48:2508–2516.

Julien S, Puig I, Caretti E, Bonaventure J, Nelles L, van Roy F, Dargemont C, de Herreros AG, Bellacosa A, Larue L. 2007. Activation of NF-kappaB by Akt upregulates Snail expression and induces epithelium mesenchyme transition. Oncogene 26:7445–7456.

Katoh M. 2005. Epithelial-mesenchymal transition in gastric cancer (Review). Int J Oncol 27:1677–1683.

Katoh M, Terada M. 1996. Overexpression of bone morphogenic protein (BMP)-4 mRNA in gastric cancer cell lines of poorly differentiated type. J Gastroenterol 31:137–139.

Kigure W, Fujii T, Sutoh T, Morita H, Katoh T, Yajima RN, Yamaguchi S, Tsutsumi S, Asao T, Kuwano H. 2013. The association of VEGF-C expression with tumor lymphatic vessel density and lymph node metastasis in patients with gastric cancer and gastrointestinal stromal tumor. Hepatogastroenterology 60:277–280.

Kopf J, Paarmann P, Hiepen C, Horbelt D, Knaus P. 2013. BMP growth factor signaling in a biomechanical context. Biofactors.

Kuga H, Morisaki T, Nakamura K, Onishi H, Noshiro H, Uchiyama A, Tanaka M, Katano M. 2003. Interferon-gamma suppresses transforming growth factor-beta-induced invasion of gastric carcinoma cells through cross-talk of Smad pathway in a three-dimensional culture model. Oncogene 22:7838–7847.

Larue L, Bellacosa A. 2005. Epithelial-mesenchymal transition in development and cancer: role of phosphatidylinositol 3′ kinase/AKT pathways. Oncogene 24:7443–7454.

Lee YC, Cheng TH, Lee JS, Chen JH, Liao YC, Fong Y, Wu CH, Shih YW. 2011. Nobiletin, a citrus flavonoid, suppresses invasion and migration involving FAK/PI3K/Akt and small GTPase signals in human gastric adenocarcinoma AGS cells. Mol Cell Biochem 347:103–115.

Li GQ, Xie J, Lei XY, Zhang L. 2009. Macrophage migration inhibitory factor regulates proliferation of gastric cancer cells via the PI3K/Akt pathway. World J Gastroenterol 15:5541–5548.

Li B, Yang Y, Jiang S, Ni B, Chen K, Jiang L. 2012. Adenovirus-mediated overexpression of BMP-9 inhibits human osteosarcoma cell growth and migration through downregulation of the PI3K/AKT pathway. Int J Oncol 41:1809–1819.

Lin HL, Chiou SH, Wu CW, Lin WB, Chen LH, Yang YP, Tsai ML, Uen YH, Liou JP, Chi CW. 2007. Combretastatin A4-induced differential cytotoxicity and reduced metastatic ability by inhibition of AKT function in human gastric cancer cells. J Pharmacol Exp Ther 323:365–373.

Liu LZ, Jing Y, Jiang LL, Jiang XE, Jiang Y, Rojanasakul Y, Jiang BH. 2011. Acacetin inhibits VEGF expression, tumor angiogenesis and growth through AKT/HIF-1alpha pathway. Biochem Biophys Res Commun 413:299–305.

Liu JF, Zhou XK, Chen JH, Yi G, Chen HG, Ba MC, Lin SQ, Qi YC. 2010. Up-regulation of PIK3CA promotes metastasis in gastric carcinoma. World J Gastroenterol 16:4986–4991.

Lv Z, Yang D, Li J, Hu M, Luo M, Zhan X, Song P, Liu C, Bai H, Li B, Yang Y, Chen Y, Shi Q, Weng Y. 2013. Bone morphogenetic protein 9 overexpression reduces osteosarcoma cell migration and invasion. Mol Cells 36:119–126.

Ma J, Sawai H, Ochi N, Matsuo Y, Xu D, Yasuda A, Takahashi H, Wakasugi T, Takeyama H. 2009. PTEN regulates angiogenesis through PI3K/Akt/VEGF signaling pathway in human pancreatic cancer cells. Mol Cell Biochem 331:161–171.

Park Y, Kim JW, Kim DS, Kim EB, Park SJ, Park JY, Choi WS, Song JG, Seo HY, Oh SC, Kim BS, Park JJ, Kim YH, Kim JS. 2008. The Bone Morphogenesis Protein-2 (BMP-2) is associated with progression to metastatic disease in gastric cancer. Cancer Res Treat 40:127–132.

Qiao M, Sheng S, Pardee AB. 2008. Metastasis and AKT activation. Cell Cycle 7:2991–2996.

Shafee N, Kaluz S, Ru N, Stanbridge EJ. 2009. PI3K/Akt activity has variable cell-specific effects on expression of HIF target genes, CA9 and VEGF, in human cancer cell lines. Cancer Lett 282:109–115.

Siegel R, Naishadham D, Jemal A. 2013. Cancer statistics, 2013. CA Cancer J Clin 63:11–30.

Singh A, Morris RJ. 2010. The Yin and Yang of bone morphogenetic proteins in cancer. Cytokine Growth Factor Rev 21:299–313.

Song G, Ouyang G, Bao S. 2005. The activation of Akt/PKB signaling pathway and cell survival. J Cell Mol Med 9:59–71.

Tahara E. 1993. Molecular mechanism of stomach carcinogenesis. J Cancer Res Clin Oncol 119:265–272.

Tapia O, Riquelme I, Leal P, Sandoval A, Aedo S, Weber H, Letelier P, Bellolio E, Villaseca M, Garcia P, Roa JC. 2014. The PI3K/AKT/mTOR pathway is activated in gastric cancer with potential prognostic and predictive significance. Virchows Arch 465:25–33.

Tian WY, Chen WC, Li R, Liu L. 2013. Markers CD40, VEGF, AKT, PI3K, and S100 correlate with tumor stage in gastric cancer. Onkologie 36:26–31.

Uyama I, Suda K, Satoh S. 2013. Laparoscopic surgery for advanced gastric cancer: Current status and future perspectives. J Gastric Cancer 13:19–25.

Wagner DO, Sieber C, Bhushan R, Borgermann JH, Graf D, Knaus P. 2010. BMPs: From bone to body morphogenetic proteins. Sci Signal 3:mr 1.

Wang LT. 1993. [Clinicopathological analysis, immunohistochemical study and electron microscopic observation of chondroblastoma of bone]. Zhonghua Wai Ke Za Zhi 31:717–721.

Wang K, Feng H, Ren W, Sun X, Luo J, Tang M, Zhou L, Weng Y, He TC, Zhang Y. 2011. BMP9 inhibits the proliferation and invasiveness of breast cancer cells MDA-MB-231. J Cancer Res Clin Oncol 137:1687–1696.

Wen YG, Wang Q, Zhou CZ, Qiu GQ, Peng ZH, Tang HM. 2010. Mutation analysis of tumor suppressor gene PTEN in patients with gastric carcinomas and its impact on PI3K/AKT pathway. Oncol Rep 24:89–95.

Yasui W, Oue N, Aung PP, Matsumura S, Shutoh M, Nakayama H. 2005. Molecular-pathological prognostic factors of gastric cancer: A review. Gastric Cancer 8:86–94.

Ye B, Jiang LL, Xu HT, Zhou DW, Li ZS. 2012. Expression of PI3K/AKT pathway in gastric cancer and its blockade suppresses tumor growth and metastasis. Int J Immunopathol Pharmacol 25:627–636.

Ye L, Kynaston H, Jiang WG. 2008. Bone morphogenetic protein-9 induces apoptosis in prostate cancer cells, the role of prostate apoptosis response-4. Mol Cancer Res 6:1594–1606.

Ye L, Lewis-Russell JM, Kyanaston HG, Jiang WG. 2007. Bone morphogenetic proteins and their receptor signaling in prostate cancer. Histol Histopathol 22:1129–1147.

Zhou BP, Liao Y, Xia W, Spohn B, Lee MH, Hung MC. 2001. Cytoplasmic localization of p21Cip1/WAF1 by Akt-induced phosphorylation in HER-2/neu-overexpressing cells. Nat Cell Biol 3:245–252.

SUPPORTING INFORMATION

Additional supporting information may be found in the online version of this article at the publisher's web-site.